High Speed Radiography Can Be Used to Measure Dynamic Spinal Cord Deformation in an *in vivo* Rodent Model

E. Lucas[1,2], J. Liu[2], C. Russell[1,2], W. Tetzlaff[2], P. Cripton[1,2]
[1] Orthopaedic Injury Biomechanics Group, Departments of Mechanical Engineering and Orthopaedics; [2] International Collaboration on Repair Discoveries (ICORD)
The University of British Columbia, Vancouver, BC, Canada

ABSTRACT

Spinal cord injuries (SCIs) are commonly studied by causing injury to rodent spinal cords in vivo and analyzing histological and behavioral results post injury. However, very few researchers have investigated the deformation of the in vivo spinal cord dynamically during impact. This knowledge would help to define relationships between impact parameters, internal structure deformation (such as grey and white matter), and histological and functional outcomes which could be used to improve SCI treatment and prevention methods. The objective of this study was to develop a method of tracking the real-time internal and surface deformations of an anesthetized rat's spinal cord during injury. Twelve Sprague Dawley rats were used for this study. After a laminectomy of C5, two radio-opaque beads were injected into the cord (one dorsal, one ventral bead) using a custom technique. Four additional beads were glued to the surface of the cord caudal and cranial to the injection site (one dorsal, one ventral). The dorsal surface of the cord was impacted using a hydraulic actuator at approximately 130mm/s to a depth of 1mm. The spine was imaged laterally at 3,000 fps using a custom high speed x-ray system and the bead motion was tracked in the x-ray video. The internal dorsal bead had significantly larger anterior displacements than the internal ventral bead (0.85 ± 0.14 vs. 0.30mm ± 0.11mm (avg±SD) respectively) and than all surface beads. The internal ventral beads had significantly larger anterior displacements than the ventral surface bead displacements. The dorsal beads had larger maximum velocities in the anterior direction than the ventral beads. The bead migration was not significant in the anterior direction, and was small in the cranial direction (approximately 0.04mm). Harvested spinal cords showed that the internal dorsal beads were in the dorsal white matter. The internal ventral beads were in the ventral white matter for half of the animals and the ventral grey matter for the remaining. There were no significant differences found between white and grey matter motion. These results indicate the merit of this technique for measuring in vivo spinal cord deformation.

INTRODUCTION

Spinal cord injuries (SCIs) are extremely debilitating injuries and affect approximately 12,000 people a year in the United States (NSCIC, 2010). It is well known that the severity of SCI is correlated with the biomechanics of impact, specifically velocity and compression (Kearney, 1988). Limited data exists however on the biomechanics of the spinal cord during impact. Some researchers have studied the biomechanics of surrogate spinal cords (Bilston and Thibault, 1997; Kroeker, 2009; Saari, 2006; Van Toen, 2008) and others have modeled it with finite element methods (Greaves, 2008; Maikos, 2008; Li and Dai, 2009; Sparrey, 2009). Such models require accurate spinal cord material properties which are typically obtained from *ex vivo* mechanical testing of human and animal spinal cords (Bilston and Thibault, 1995; Fiford and Bilston, 2005; Oakland, 2006; Jones, 2008). The spinal cord's material properties are known to change quickly after death, necessitating *in vivo* testing for accurate characterization (Oakland, 2006). *In vivo* animal models have been widely used to study SCIs, however research is typically focused on post-injury results such as histology, behavioral assessment, and the effectiveness of treatments. There is a paucity of studies evaluating how the cord moves during impact. The various components of the spinal cord (i.e. white and grey matter) may have different material properties and they thus may move differently under impact (Ichihara, 2001). Understanding the biomechanics of the structure and subcomponents of the spinal cord can give insight into the histology and behavioral results and help validate existing models of the spinal cord. This enhanced knowledge of the interactions between impact parameters, spinal cord biomechanics, and injury can help improve surgical treatments and preventative methods.

The limited research on spinal cord biomechanics is due in part to complications of implementing appropriate imaging techniques to record spinal cord deformations during injury. Hung et al. used a high speed camera to image *in vivo* spinal cord movement of a cat during a SCI, however this approach required a large laminectomy and it could not show internal tissue deformation (Hung, 1975). MRI has been used to study spinal cord tissue level injury after experimental SCI in rodents (Bilgen, 2001; Gareau, 2001); however, MRI cannot capture the dynamic nature of a single injurious high speed impact. High speed x-ray has been used to image animal and cadaveric human specimens during biomechanical tests (Al-Bsharat, 1999; Bauman and Chang, 2010; Brainerd, 2010; Sundararajan, 2004; Ono, 1997; Martin, 2010). It is a promising method for imaging spinal cord motion during a SCI but does require the inclusion of radio-opaque fiducial marker in the cord since neural tissue is radio-translucent. Mainman et al. injected contrast agent into the spinal cord of an *in vivo* cat and imaged the displacement of the spinal cord during impact with x-ray; however, this was not x-rayed at high speeds and only a single marker was injected in each spinal cord segment giving limited information on the dynamic deformation of the cord (Maiman, 1989). There is a need to develop a technique for imaging high speed motion of several fiducials in an *in vivo* spinal cord as this will allow calculation of the deformation of multiple components in the spinal cord during impact.

The objectives of this study were to (1) develop a method of using high speed x-ray to track internal and surface deformations of an *in vivo* rat spinal cord at high collection rates during SCI and (2) collect initial surface and internal spinal cord deformation data during a typical experimental contusion injury.

METHODS

Twelve anesthetized Sprague Dawley rats were used for this study, which was approved by the UBC Animal Care Centre and Ethics Committee. Radio-opaque Tantalum beads (260µm diameter) were used as fiducials to measure movement and deformation of the spinal cord tissue during impact. A full laminectomy of C5 was performed to expose the dorsal and lateral sides of the spinal cord in this area. One bead was injected into the dorsal cord, about 0.6mm below the surface, and another was injected into the ventral cord, about 2.1mm below the surface (Figure 1). The required injection depth and angle were determined using a rat spinal cord atlas (Paxinos and Watson, 1986), and these injection locations were intended to be in the approximate location of the dorsal and ventral white matter. To inject the beads, a channel was first created in the spinal cord to the desired bead location using a 350µm diameter needle. The bead was then placed on top of the channel and pushed to the bottom using a 30 gauge needle (300µm) with a flattened tip. Four additional beads were glued to the surface of the cord caudal and cranial to the injection site through small holes made in the dura. Since the internal beads were not directly glued to the spinal cord, it was necessary to verify that these beads were not migrating with respect to the spinal cord during impact. If the injected beads' post-impact displacements were greater than the glued surface beads, then we attributed the difference to bead migration. A 1.0mm bead was glued to the transverse process of C5 to measure spinal column motion. All bead displacements were normalized to this reference bead. The scapulas were also removed since this was a non-survival study and they interfered with bead visualization.

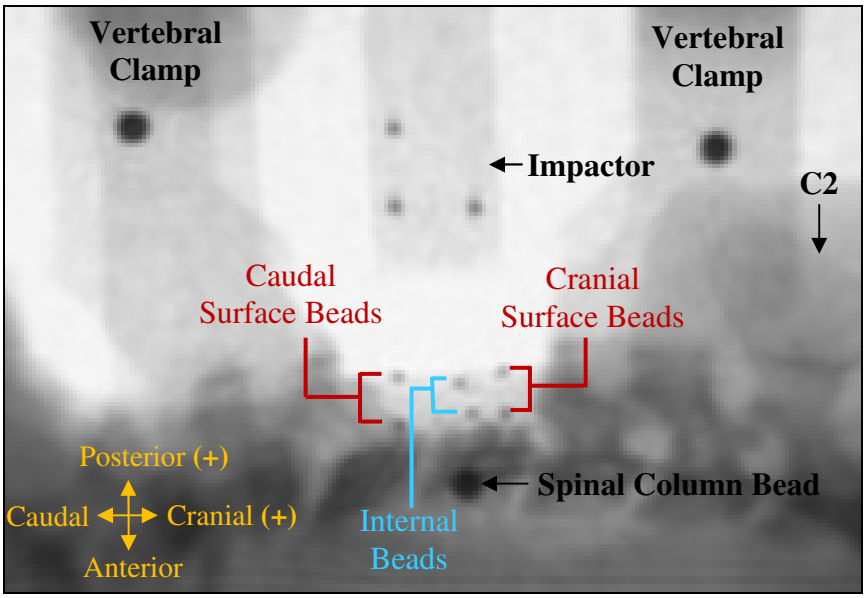

Figure 1: Lateral high speed x-ray image showing bead positioning in the cervical spinal cord of an anesthetized rat. Internal beads were in the dorsal and ventral internal aspects of the cord. Surface beads were on the ventral and dorsal aspects of the cord both cranial and caudal to the internal beads.

The spine was stabilized by clamping C3&C4 and C6&C7 and fixing them to the test frame using articulating arms. The spinal cord was impacted at C5 at 130mm/s to a depth of 1mm (similar to Infinite Horizons (Scheff, 2003)) using a 4mm x 2.5mm impactor attached to a hydraulic actuator (Instron Dynamight). The impactor was first lowered until it touched the dura

of the spinal cord (verified visually) and was then raised above the surface of the spinal cord and accelerated downwards to 1.0mm past the dura contact position. The impact was imaged laterally with high speed x-ray (40kV and 2ma) at 3,000 frames per second. Force and acceleration data were collected at 20kHz from a 5N load cell and 50G accelerometer attached to the actuator and impactor. The force was inertially compensated using the accelerometer data. The rat was euthanized immediately after impact. The spinal cord was then harvested, fixed in 4% Paraformaldehyde, and dissected to determine the internal bead locations (dorsal or ventral, white or grey matter).

The x-ray video was undistorted using XROMM software (Brainerd, 2010), and denoised using custom 3D curvelet image denoising software, making use of the CurveLab toolkit (Candes, 2006). The bead motion, impactor motion, and clamp motion were tracked in the cranial and anterior directions using TEMA Motion software (Image Systems) and filtered with a 300Hz 4^{th} order Butterworth filter. The mm/pixel conversion factor was calculated by dividing the average actuator displacement from the actuator's LVDT data by the tracked impactor displacement in pixels from beads glued to the impactor.

The bead tracking precision was estimated by averaging the variation of the spinal cord bead displacement before impact, when the beads are at rest. The bead tracking accuracy was determined by imaging ten additional impacts with high speed x-ray without an animal present. A 260µm Tantalum bead was glued to a piece of plastic attached to the tip of the impactor and was cover with a segment of a cadaveric rat spinal cord. The bead displacement was tracked, converted to mm, and compared to LVDT data to assess the tracking accuracy.

A repeated measures ANOVA was performed on the bead impact displacements, velocities, and permanent displacements of the impact tests with bead position (i.e. internal dorsal, cranial dorsal, caudal ventral, etc.) as the factor. A Student Newman Keuls post-hoc test was performed to identify significance between beads. The bead displacements for the accuracy study were analyzed in the same manor. A matched pairs t-test was performed for assessing white versus grey matter motion, with the internal bead location (white or grey matter) as a categorical factor.

RESULTS

The rats tolerated the bead injections and showed no respiratory or cardiac changes. The beads could be successfully injected into the dorsal and ventral spinal cord. The bead motion was visible with high speed x-ray after denoising and undistortion and successfully tracked. The average force of impact was 1.28N ± 0.3N and the average impact velocity was 131.6mm/s ± 1.3mm/s (avg±STD).

At maximum compression, the internal dorsal bead had approximately 65% larger anterior displacement than the internal ventral bead ($p<0.0002$) and 14%-94% larger anterior displacement than all of the surface beads ($p<0.02$) (Table 1). The internal ventral bead also had 54%-70% larger anterior displacement than the ventral surface beads ($p<0.0002$). These trends are also evident when looking at the average bead displacements over time during impact (Figure

2). In the cranial direction, the internal dorsal bead moved more than all of the surface beads ($p<0.04$) and the internal ventral bead moved more than the caudal dorsal/ventral and cranial ventral surface beads ($p<0.02$).

Table 1: Average spinal cord bead displacements at maximum compression, maximum velocities during impact, and permanent displacement after impact (avg±STD).

	Displacement at Maximum Compression (mm)		**Maximum Velocity During Impact (mm/s)**		**Permanent Displacement (mm)**	
Bead	**C/C Direction**	**A/P Direction**	**C/C Direction**	**A/P Direction**	**C/C Direction**	**A/P Direction**
Caudal Dorsal	0.06 ± 0.10	-0.62 ± 0.24	10.33 ± 15.28	84.45 ± 30.21	-0.01 ± 0.06	-0.10 ± 0.10
Cranial Dorsal	0.12 ± 0.12	-0.73 ± 0.14	17.00 ± 19.96	92.79 ± 22.84	0.01 ± 0.08	-0.11 ± 0.09
Internal Dorsal	0.19 ± 0.14	-0.85 ± 0.13	22.79 ± 14.28	99.89 ± 12.48	0.04 ± 0.07	-0.09 ± 0.10
Caudal Ventral	0.09 ± 0.04	0.05 ± 0.10	11.84 ± 11.71	-5.11 ± 18.64	0.02 ± 0.05	-0.02 ± 0.07
Cranial Ventral	0.08 ± 0.08	0.07 ± 0.14	13.43 ± 19.18	-12.46 ± 16.15	0.02 ± 0.07	-0.03 ± 0.09
Internal Ventral	0.20 ± 0.18	-0.30 ± 0.11	18.68 ± 20.26	38.51 ± 14.57	0.05 ± 0.07	-0.01 ± 0.08

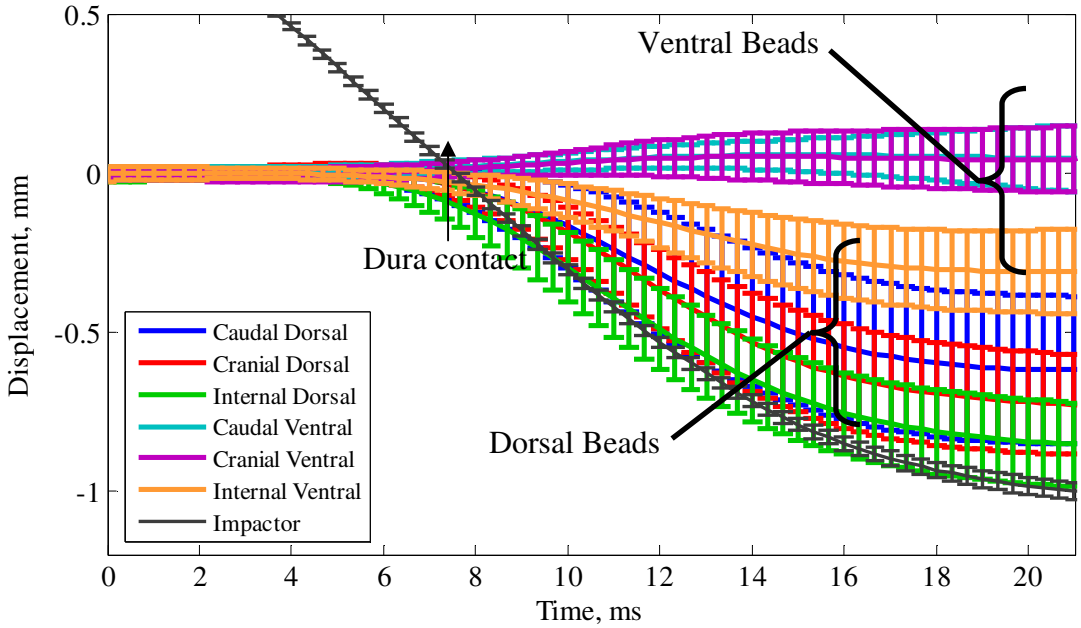

Figure 2: Spinal cord bead displacements during impact (avg±STD). The end of the data series represents maximum compression displacement recorded in Table 1.

To determine bead velocity, a cubic spline was fit to the displacement data and the resulting curve was differentiated (Appendix A). During impact, the internal dorsal bead had significantly larger maximum velocities in the anterior direction than the internal ventral bead ($p<0.0002$) and ventral surface beads ($p<0.0002$) but no significant difference with the dorsal surface beads ($p=0.1$) (Table 1). The internal ventral bead had significantly larger maximum velocities than the ventral surface beads ($p<0.0002$). There were no significant differences in the maximum bead velocities in the cranial/caudal direction ($p=0.2$).

In the anterior direction, there were no significant differences in the permanent displacement of the internal dorsal bead compared to the dorsal surface beads ($p=0.4$), as well as the internal ventral bead compared to the ventral surface beads ($p=0.5$) (Table 1). In the cranial direction the internal dorsal bead had significantly higher permanent displacements than the dorsal surface beads ($p<0.03$), with an average displacement about 0.04mm greater than the surface bead averages. The internal ventral bead also had significantly higher permanent displacements than the ventral surface beads ($p<0.003$), which was also about 0.04mm greater than the surface beads.

The bead tracking precision, defined in this study as the mean standard deviation of the bead movement when the beads were at rest, was 0.021mm ± 0.01mm. For the bead tracking accuracy study the average difference between the LVDT and the internal spinal cord bead displacement was 0.019 ± 0.044mm, although this difference was not statistically significant ($p=0.9$).

Harvested spinal cords showed the internal dorsal beads were in the dorsal white matter and the internal ventral beads were in the ventral white matter for half of the animals and the ventral grey matter for the remaining. There were no significant differences between the grey and white matter internal ventral beads for maximum displacement, velocity, and permanent displacement ($p=0.4$).

DISCUSSION

The results indicate the merit of this technique for measuring *in vivo* spinal cord deformation. A crucial step in validating this methodology was verifying that the internal markers did not migrate with respect to the spinal cord tissue during the impact. Many researchers that have used radio-opaque fiducial markers in neural and orthopaedic tissue assume the markers do not move independently of the tissue (Brainerd, 2010; Maiman, 1989; Panjabi, 2000). While this is probably a valid assumption for markers glued to tissue or bone, migration of markers not rigidly affixed should be evaluated. Hardy et al. tracked the motion of brain tissue using neutral density targets (NDTs) of a similar density to neural tissue to reduce the chance of migration (Hardy et. al, 2001). Migration of the NDTs was assessed by comparing the marker locations before and after impact. The current study also assumes that any bead migration would permanently displace the bead from its original position post-impact. Any post-impact displacement greater than the permanent cord deformation (surface bead post-impact displacement) was attributed to bead migration. There was no significant migration in the anterior direction but there was slight migration in the cranial direction. It is possible that the internal spinal cord tissue experiences more movement than the surface of the spinal cord due to pressure waves after impact. If this is true, what has been deemed as migration may actually be permanent deformation of the internal tissue that has exceeded the surface tissue deformation. The inherent limitation of this approach is that the spinal cord tissue cannot be seen in x-ray so it is not known definitively whether post-impact displacement is a good predictor of migration. Further validation is being considered including finite element modeling and/or MRI validation.

The differences in bead displacements and velocities imply that the spinal cord undergoes complex internal and surface deformations during impact. The larger displacements and higher

velocities of the dorsal beads versus the ventral beads in the anterior direction is most likely because the spinal cord was impacted at the dorsal surface. The energy from the impact would dissipate as it travels through the spinal cord, causing less movement in the ventral cord. The larger displacement of the internal ventral bead versus ventral surface beads in the anterior direction may be due to structural differences of the internal cord and the surface, allowing more movement in the interior. The greater displacement of the internal beads versus the surface beads in the cranial direction could be due to pressure waves within the spinal cord during impact.

The differences in white matter and grey matter material properties are currently debated in published studies (Ichihara, 2001; Ozawa, 2001). While there was not a significant difference seen between ventral white and grey matter motion in this study, further studies are needed with larger animal numbers and more bead locations to quantitatively examine the question of white versus grey matter motion. A larger animal model is recommended for this type of study to allow for more localized marker positions and finer detection of differences in the white and grey matter. Many applications of this technique are conceivable including comparing localized grey and white matter motion during impact to histological findings. This could help explain phenomenon such as "white matter sparring" and large grey matter damage after a SCI (Choo, 2007).

A limitation of this technique is the need to inject beads into the spinal cord. The damage was investigated by harvesting the spinal cords of non-injured animals with bead injections. While damage was seen along the injection track, it appeared to be minimal and was smaller than the diameter of the bead. The injection of the beads creates a small hole in the dura, which could affect the movement of the spinal cord due to pressure loss in the CSF which has protective qualities. It was noticed that only a small amount of CSF was lost during injection. A full laminectomy was performed with this study because a large area of the spinal cord was being impacted and the methodology was in its developmental stages. If it is only desired to impact one spinal cord segment, the beads could be injected between two laminae by removing the ligaments and hanging a small weight on the tail to increase the intervertebral space, thereby preventing the need of the laminectomy. Another potential limitation is the possibility that the spinal cord moves differently with bead inclusions. The current study assumes that the beads are small enough to not alter the spinal cord mechanics, however this could be further investigated with finite element models, surrogate cord models, and/or repeated in vivo or ex vivo experimental measurements.

CONCLUSIONS

A method was successfully developed to measure *in vivo* rat spinal cord biomechanics using high speed x-ray. Bead migration during impact was shown to be small and mostly insignificant. Results showed differences in displacements and velocities of beads inside of the spinal cord and on the surface of the cord, suggesting that the spinal cord moves in a complex non-uniform manner. Future applications of this technique involve investigating white versus grey matter movement, comparing bead movements with histology and behavioral outcomes, and validating of spinal cord models. This information would improve our knowledge on the basic science behind how the spinal cord becomes injured and could be used to improve existing clinical treatments and preventative measures.

ACKNOWLEDGEMENTS

We gratefully acknowledge the Canadian Institutes for Health Research for funding this work and the Centre for Hip Health and Mobility for providing access to the high speed x-ray apparatus.

REFERENCES

Al-Bsharat, A. S., W. N. Hardy, et al. (1999). "Brain/Skull Relative Displacement Magnitude Due to Blunt Head Impact: New Experimental Data and Model." Proceedings of the 43rd Stapp Car Crash Conference; San Diego, California, SAE International.

Bauman, J. M. and Y.-H. Chang (2010). "High-speed X-ray video demonstrates significant skin movement errors with standard optical kinematics during rat locomotion." Journal of Neuroscience Methods **186**(1): 18-24.

Bilgen, M., R. Abbe, et al. (2001). "Dynamic contrast-enhanced MRI of experimental spinal cord injury: in vivo serial studies." Magn Reson Med **45**(4): 614-22.

Bilston, L. E. and L. E. Thibault (1995). "The mechanical properties of the human cervical spinal cord in vitro." Ann Biomed Eng **24**(1): 67-74.

Bilston, L. E. and L. E. Thibault (1997). "Biomechanics of cervical spinal cord injury in flexion and extension: a physical model to estimate spinal cord deformations." International Journal of Crashworthiness **2**(2): 207-218.

Brainerd, E. L., D. B. Baier, et al. (2010) "X-ray reconstruction of moving morphology (XROMM): precision, accuracy and applications in comparative biomechanics research." J Exp Zool A Ecol Genet Physiol (E-pub ahead of print).

Candes, E., et al. (2006). "Fast discrete curvelet transforms." Society for Industrial and Applied Mathematics **5**(3): 861-899.

Choo, A. M., J. Liu, et al. (2007). "Contusion, dislocation, and distraction: primary hemorrhage and membrane permeability in distinct mechanisms of spinal cord injury." J Neurosurg Spine **6**(3): 255-66.

Fiford, R. J. and L. E. Bilston (2005). "The mechanical properties of rat spinal cord in vitro." J Biomech **38**(7): 1509-15.

Gareau, P. J., L. C. Weaver, et al. (2001). "In vivo magnetization transfer measurements of experimental spinal cord injury in the rat." Magn Reson Med **45**(1): 159-63.

Greaves, C. Y., M. S. Gadala, et al. (2008). "A three-dimensional finite element model of the cervical spine with spinal cord: an investigation of three injury mechanisms." Ann Biomed Eng **36**(3): 396-405.

Hardy, W. N., C. D. Foster, et al. (2001). "Investigation of Head Injury Mechanisms Using Neutral Density Technology and High-Speed Biplanar X-ray." Stapp Car Crash J **45**: 337-68.

Hung, T. K., M. S. Albin, et al. (1975). "Biomechanical responses to open experimental spinal cord injury." Surg Neurol **4**(2): 271-6.

Ichihara, K., T. Taguchi, et al. (2001). "Gray matter of the bovine cervical spinal cord is mechanically more rigid and fragile than the white matter." J Neurotrauma **18**(3): 361-7.

Jones, C. F., S. G. Kroeker, et al. (2008). "The effect of cerebrospinal fluid on the biomechanics of spinal cord: an ex vivo bovine model using bovine and physical surrogate spinal cord." Spine (Phila Pa 1976) **33**(17): E580-8.

Kearney, P. A., S. A. Ridella, et al. (1988). "Interaction of contact velocity and cord compression in determining the severity of spinal cord injury." J Neurotrauma **5**(3): 187-208.
Kroeker, S. G., P. L. Morley, et al. (2009). "The development of an improved physical surrogate model of the human spinal cord--Tension and transverse compression." Journal of Biomechanics **42**(7): 878-883.
Li, X. F. and L. Y. Dai (2009). "Three-dimensional finite element model of the cervical spinal cord: preliminary results of injury mechanism analysis." Spine (Phila Pa 1976) **34**(11): 1140-7.
Maikos, J. T., Z. Qian, et al. (2008). "Finite element analysis of spinal cord injury in the rat." J Neurotrauma **25**(7): 795-816.
Maiman, D. J., J. Coats, et al. (1989). "Cord/spine motion in experimental spinal cord injury." J Spinal Disord **2**(1): 14-9.
Martin, D. E., N. J. Greco, et al. (2010). "Model-Based Tracking of the Hip: Implications for Novel Analyses of Hip Pathology." J Arthroplasty (E-pub ahead of print).
National Spinal Cord Injury Statistics Center, NSCIS. (2010). "Spinal Cord Injury Facts and Figures at a Glance." Retrieved February, 2010, from www.nscisc.uab.edu.
Oakland, R. J., R. M. Hall, et al. (2006). "The biomechanical response of spinal cord tissue to uniaxial loading." Proc Inst Mech Eng [H] **220**(4): 489-92.
Ono K, Kaneoka K, Wittek A, et al. (1997). "Cervical injury mechanism based on the analysis of human cervical vertebral motion and head-neck-torso kinematics during low speed rear impacts." 41st STAPP Car Crash Conference; Lake Buena Vista, Florida, 1997:339-56.
Ozawa, H., T. Matsumoto, et al. (2001). "Comparison of spinal cord gray matter and white matter softness: measurement by pipette aspiration method." J Neurosurg **95**(2 Suppl): 221-4.
Panjabi, M. M., T. Oda, et al. (2000). "The effects of pedicle screw adjustments on neural spaces in burst fracture surgery." Spine (Phila Pa 1976) **25**(13): 1637-43.
Paxinos, G. and C. Watson (1986). The Rat Brain in Stereotaxic Coordinates: Second Edition, Academic Press, Inc.
Saari A, Itshayek E, Nelson TS, Morley, P.L.; Cripton, P.A. (2006). "Spinal Cord Deformation During Injury of the Cervical Spine in Head-First Impact." Proceedings of the International Research Council on the Biomechanics of Impacts ; 2006 Annual Meeting, Madrid, Spain.
Scheff, S. W., A. G. Rabchevsky, et al. (2003). "Experimental modeling of spinal cord injury: characterization of a force-defined injury device." J Neurotrauma **20**(2): 179-93.
Sparrey, C. J., G. T. Manley, et al. (2009). "Effects of white, grey, and pia mater properties on tissue level stresses and strains in the compressed spinal cord." J Neurotrauma **26**(4): 585-95.
Sundararajan, S., P. Prasad, et al. (2004). "Effect of Head-Neck Position on Cervical Facet Stretch of Post Mortem Human Subjects during Low Speed Rear End Impacts." Stapp Car Crash J **48**: 331-72.
Van Toen (Née Greaves) C, Nelson TS, Jones CF, Street J, Cripton PA. (2008). "Development of an *in vitro* model of head-first impact with a hybrid III head, surrogate spinal cord and simulated neck muscles." Proceedings of the NHTSA 36th International Workshop on Human Subjects for Biomechanical Research; November 2, 2008, San Antonio, USA**.**

APPENDIX A

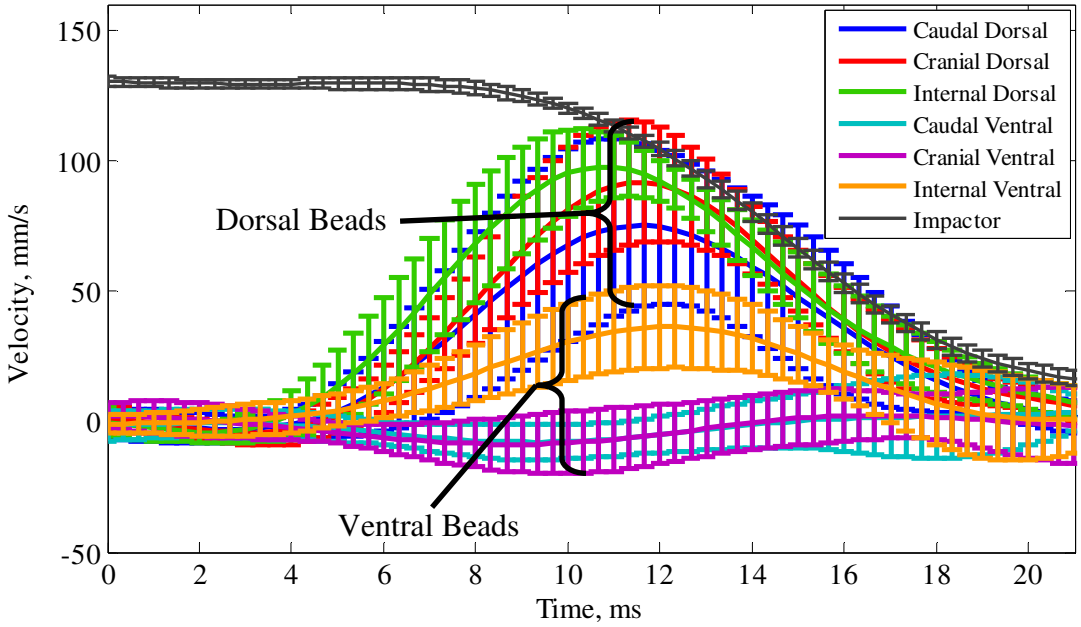

Figure A: Spinal cord bead velocities during impact (avg±STD). The maximum values represent the data recorded in Table 1.

AUTHOR LIST

1. Erin Lucas
   Blusson Spinal Cord Centre
   5000/818 West 10th Ave
   Vancouver, BC V5Z 1L8
   Canada
   (604) 675-8845
   elucas@interchange.ubc.ca

2. Jie Liu
   Blusson Spinal Cord Centre
   5000/818 West 10th Ave
   Vancouver, BC V5Z 1L8
   Canada
   (604) 675-8505
   jliu@icord.org

3. Colin Russell
   Blusson Spinal Cord Centre
   5000/818 West 10th Ave
   Vancouver, BC V5Z 1L8
   Canada
   (604) 675-8845
   crussell@interchange.ubc.ca

4. Wolfram Tetzlaff
   Blusson Spinal Cord Centre
   5530/818 West 10th Ave
   Vancouver, BC V5Z 1L8
   Canada
   (604) 675-8848
   tetzlaff@icord.org

5. Peter Cripton
   Blusson Spinal Cord Centre
   5430/818 West 10th Ave
   Vancouver, BC V5Z 1L8
   Canada
   (604) 822-6629
   cripton@mech.ubc.ca